An experimental study of the biological impact of a superflare on the TRAPPIST-1 planets

X. C. Abrevaya,[1,2,3,*★] P. Odert,[3†] O. J. Oppezzo,[4,*] M. Leitzinger,[3] G. J. M. Luna,[5,6,*] E. Guenther,[7] M. R. Patel,[8] and A. Hanslmeier [3]

[1] *Instituto de Astronomía y Física del Espacio (UBA - CONICET), Ciudad Autónoma de Buenos Aires, Argentina*
[2] *Facultad de Ciencias Exactas y Naturales, Universidad de Buenos Aires, Ciudad Autónoma de Buenos Aires, Argentina*
[3] *Institute of Physics, Department of Astrophysics & Geophysics, University of Graz, Austria*
[4] *Departamento de Radiobiología, Comisión Nacional de Energía Atómica. Buenos Aires, Argentina*
[5] *Universidad Nacional de Hurlingham (UNAHUR), Secretaría de Investigación, Av. Gdor. Vergara 2222, Villa Tesei, Buenos Aires, Argentina*
[6] *Consejo Nacional de Investigaciones Científicas y Técnicas (CONICET)*
[7] *Thüringer Landessternwarte Tautenburg, Sternwarte 5, 07778 Tautenburg, Germany*
[8] *School of Physical Sciences, The Open University, Milton Keynes, MK7 6AA, U.K.*
[*] *Members of the Argentinian Research Unit in Astrobiology*

Accepted XXX. Received YYY; in original form ZZZ

ABSTRACT

In the present study, we conducted experiments to assess the biological effects of high fluences of UV radiation (UVR) on the TRAPPIST-1 planetary system (planets e, f, g within the habitable zone), unlike previous estimates made by other authors which used theoretical approaches. To this end, we first calculated the UV fluxes at the orbits of the planets of the TRAPPIST-1 system during quiescent conditions and during a superflare. We then studied the effects of UVR on microbial life by exposing UV-tolerant (*Deinococcus radiodurans*) and UV-susceptible bacteria (*Escherichia coli*) to fluences equivalent to a superflare on the unshielded surface of these planets. Based on the results of our laboratory experiments, we have found a survival fraction of 6.31×10^{-8} for *D. radiodurans* and a survival fraction below the limit of detection for *E. coli* at the surface of the planet e, which would receive the highest UVR flux. These survival fractions were higher for the planets f and g. In contrast to the results obtained by other authors which used theoretical estimates, we show that a fraction of the population of microorganisms could tolerate the high UVR fluences of a superflare on the surface of TRAPPIST-1 planets, even without any shielding such as that provided by an atmosphere or an ocean. Our study evidences the existence of methodological problems in theoretical approaches. It also emphasizes the importance of performing specifically designed biological experiments to predict microbial survival in extraterrestrial contexts.

Key words: Astrobiology – Planets and satellites: terrestrial planets – Planets and satellites: surfaces – Stars: flare – Stars: activity – Ultraviolet: stars

1 INTRODUCTION

The TRAPPIST-1 planetary system is composed of seven terrestrial-like planets (b, c, d, e, f, g, and h) that orbit a nearby (~12 pc) ultra-cool M8 dwarf star, TRAPPIST-1 (Gillon et al. 2016, 2017). Planets b, c, e, f, and g are Earth-sized planets whereas d and h have sizes between Earth and Mars (Agol et al. 2021). Three of these planetary bodies are in the conservative liquid water habitable zone (LW-HZ), namely planets e, f, and g, and therefore are considered potentially habitable (Gillon et al. 2017), although many other factors would be required to assess their potential to host life.

Planets e, f, and g could harbor water oceans on their surfaces assuming Earth-like atmospheres, but planets b, c, and d could only have limited regions of liquid water on their surfaces (Gillon et al. 2017). The TRAPPIST-1 planetary atmospheres have been probed with transmission spectroscopy. No absorption signatures in the transmission spectra obtained by the Hubble Space Telescope (HST) have been reported so far and the existence of hydrogen-rich extended atmospheres has been ruled out by observations (de Wit et al. 2016; Zhang et al. 2018; Ducrot et al. 2018; Burdanov et al. 2019; Gressier et al. 2022) as well as by theoretical investigations (Hori & Ogihara 2020). If the planets could have atmospheres, the two outermost may retain atmospheres on Gyr timescales (Dong et al. 2018). Several studies have argued for the James Webb Space Telescope (JWST) having the sensitivity and potential to detect

★ E-mail: abrevaya@iafe.uba.ar
† E-mail: petra.odert@uni-graz.at

more compact atmospheres (e.g. Lustig-Yaeger et al. 2019; Pidhorodetska et al. 2020). However, first transmission spectroscopic observations revealed the problem of stellar contamination (Lim et al. 2023) in the form of e.g. star spots and/or faculae. Therefore, planetary atmospheric signals could not yet be confirmed. Also, observations during the secondary eclipse with JWST by Ih et al. (2023); Zieba et al. (2023) provided constraints on the planetary atmospheric scenarios, favouring either a bare rock surface or a thin, O_2-dominated low-CO_2 atmosphere. Lincowski et al. (2023) tested further planetary atmospheric scenarios of planet *c*, where low-pressure O_2 atmospheres with few CO_2 are as well possible, but 10% of H_2O also seem to be compatible with the data. Very recently, Van Looveren et al. (2024) modeled atmospheric loss rates of N_2-CO_2 atmospheres for the TRAPPIST-1 planet system, concluding that even at present irradiation levels no significant atmospheres could be maintained over extended timescales. For recent reviews on the TRAPPIST-1 planetary system and atmospheres, we refer the reader to Turbet et al. (2020) and Gillon (2024).

This planetary system orbits the star TRAPPIST-1, a very late, cool, and old but still active dM star. TRAPPIST-1 has a mass close to the hydrogen burning limit. Our Sun is approximately eleven times more massive, ~2000 times more luminous, and its radius is roughly eight times larger than TRAPPIST-1 (detailed parameters are given in Van Grootel et al. 2018). TRAPPIST-1 has an age of 7.6±2.2 Gyr (Burgasser & Mamajek 2017). The X-ray luminosity of TRAPPIST-1 is similar to that from the quiescent Sun (6×10^{26}erg s^{-1}, Wheatley et al. 2017) and given that the bolometric luminosity of TRAPPIST-1 is much lower than that from the Sun, this is remarkable. The flare activity of TRAPPIST-1 was investigated by Vida et al. (2017). In the *Kepler* K2 light curve, 42 flares have been identified, leading to a flare rate of about one flare in two days. The K2 flares have energies in the range of $10^{30...33}$ erg, with one flare out of 42 being a superflare.

The question of habitability in the TRAPPIST-1 planetary system was studied by Wolf (2017) using 3D climate modeling. It has been found that planet *e* is likely the most suitable to support a habitable environment, with Earth-like surface temperatures and possibly liquid water oceans. This finding has been confirmed by Dobos et al. (2019) by investigating tidal heating on the four inner planets. They have found that planets *d* and *e* can avoid a runaway greenhouse phase. As planets *f*, *g*, and *h* are too far from the star to experience significant tidal heating, Dobos et al. (2019) also suggested that these planets may likely have solid ice surfaces with possible subsurface liquid water oceans. Thus, according to these studies, the best candidate for being habitable would be planet *e*. However, Kislyakova et al. (2017) postulated the potential existence of magnetic induction heating which might lead to enhanced volcanism and outgassing on planet *e*. Very recently, Payne & Kaltenegger (2024) found that planets *e*, *f*, *g*, and *h* could be warm enough if there is some increase in pCO2, with respect to the modern Earth value.

Given the interest in unveiling the habitability conditions of the TRAPPIST-1 planetary system, recent studies started to explore the biological impact of UV radiation (UVR) from flares in the TRAPPIST-1 system (O'Malley-James & Kaltenegger 2017; Estrela et al. 2020). To this end, these authors considered the microorganisms *Deinococcus radiodurans* (*D. radiodurans*) and *Escherichia coli* (*E. coli*) and employed parameters such as the "UV dosage for 10% survival" (F_{10}) also known as "lethal dose 90" (LD−90) to determine the chances of survival of microbial life after a flaring event. These parameters were obtained from experiments reported in the literature that were performed using fluences and fluence rates much lower than those that the microorganisms would have received from a flare or superflare on the surface of a planetary body in the TRAPPIST-1 system.

The first part of the present study is dedicated to performing a calculation of the UV spectra for the superflare of TRAPPIST-1 published by Vida et al. (2017) and estimating the UV fluxes at the surface of the planets orbiting in the LW-HZ (planets *e*, *f*, and *g*). In the second part, we performed biological experiments where we used UVR fluence rates/fluences comparable to those that the microorganisms would have received on the surface of the planets, providing a more realistic view of the eventual ability of microbial life to cope with high energetic UVR emissions from flares and superflares.

Taking into account the aforementioned, this study aims to experimentally investigate the biological impact of UVR on the surface of the potentially habitable planets *e*, *f*, and *g* of the TRAPPIST-1 system, within the frame of the EXO-UV program, an international collaborative effort that seeks to improve and expand the characterization of the UV surface habitability of exoplanets (Abrevaya et al. 2014).

2 METHODS

2.1 Estimation of UV surface fluxes during quiescent stellar conditions

Measurements of the UV emission of TRAPPIST-1 are very limited. It was observed with the *Swift* Ultraviolet/Optical Telescope (UVOT) using the *uvw2* filter, yielding a mean flux at the Earth of 8.4×10^{-18} W m^{-2} at around 190 nm (Becker et al. 2020), which corresponds to about 0.07 W m^{-2} at the orbit of planet e adopting the Gaia DR2 distance of 12.43 pc (Gaia Collaboration et al. 2018) and the orbital distance given in Gillon et al. (2017). The star remained undetected both with the *XMM-Newton* Optical Monitor in one U-band (~350 nm) observation (Obs-ID: 0743900401) and the Galaxy Evolution Explorer (*GALEX*) survey, where for the latter Loyd et al. (2020) derived upper limits to its FUV (135-178 nm) and NUV (177-273 nm) fluxes that correspond to <0.25 and <0.31 W m^{-2}, respectively, at the orbit of planet e. Recently, Wilson et al. (2021a) presented *HST* observations that also cover the UV range, but there is a data gap between about 210 and 280 nm, i.e. affecting most of the UV-C range which can be particularly biologically relevant. Therefore, we estimate the quiescent UV fluxes of TRAPPIST-1 from the reconstructed spectrum of Lincowski et al. (2018)[1]. It consists of a model spectrum (PHOENIX 2.0 with 2500 K, [Fe/H]=0, log g=5.0, scaled to the star's bolometric luminosity of $5.24\times10^{-4}L_{\odot}$) merged with a properly scaled spectrum of the M dwarf Proxima Cen below ~300 nm. The provided data is scaled to 1 AU, so we integrate the fluxes over the different UV ranges (UV-A: 315-400 nm, UV-B: 280-315 nm, UV-C: 200-280 nm) and scale them to the orbits of the planets e, f, and g, using the orbital distances given in Table 1. The given fluxes are top-of-atmosphere values, which are equivalent to surface fluxes if no atmospheric shielding is assumed. We note that other reconstructions of TRAPPIST-1's spectral energy distribution have been published subsequently (Peacock et al. 2019; Wilson et al. 2021b). Cooke et al. (2023) discussed the differences between these reconstructions and their implications for photochemical modeling of the planetary atmospheres in the TRAPPIST-1 system, as the

[1] http://vpl.astro.washington.edu/spectra/stellar/trappist1.htm

difference in the UV range (~200-400 nm) is more than two orders of magnitude. The reconstruction we adopt (Lincowski et al. 2018) lies approximately in between these extremes. However, as the UV flare fluxes we extrapolate are based on the K2 superflare, the quiescent values from all published reconstructions are still much smaller than the superflare emissions we estimate in Section 2.2.

2.2 Estimation of UV surface fluxes during a superflare

For our study, we selected a superflare of TRAPPIST-1 detected in K2 observations, as also used in Estrela et al. (2020). It has an estimated energy of 1.24×10^{33} erg and a peak flux increase of 1.78 mag in the *Kepler* photometric band (Vida et al. 2017). We note that the later analysis of the same K2 data by Paudel et al. (2018) yields a slightly lower flare energy of 7.2×10^{32} erg for this event, close to but slightly below the superflare regime ($>10^{33}$ erg). As the conversion from the *Kepler* band to white-light or bolometric energy depends on different assumptions and methods, we re-estimate its energy in section 2.2.2 with our approach and obtain a bolometric energy in the superflare regime. As the *Kepler* band ranges from ~400 to 900 nm and therefore does not cover the UV range, we estimate the UV fluxes using a blackbody model for the superflare.

2.2.1 *Peak fluxes*

It is well established that the observed spectral energy distribution of the white-light continuum emission of flares can be approximated by a hot (~8000-10000 K) blackbody both on the Sun (Castellanos Durán & Kleint 2020) and other stars (e.g. Hawley & Fisher 1992; Hawley et al. 2003; Howard et al. 2020). Thus, to obtain the UV fluxes during the peak of the TRAPPIST-1 superflare, we add a blackbody component to the quiescent spectrum of the star, yielding $F(\lambda) = F_{\rm quiet}(\lambda) + F_{\rm flare}(\lambda)$, with $F_{\rm flare}(\lambda) = X(R_*/d)^2 \pi B(\lambda, T_{\rm flare})$ (cf. Hawley et al. 2003). Here, X is the area of the flare relative to the visible hemisphere of the star, R_* is the star's radius, d the distance, and $B(\lambda, T_{\rm flare})$ the blackbody function at the flare temperature $T_{\rm flare}$. The stellar radius of $0.117 R_\odot$ is taken from Gillon et al. (2017) and the quiescent spectrum, $F_{\rm quiet}(\lambda)$, from Lincowski et al. (2018). Although the UV fluxes in this reconstructed spectrum have not been directly measured but scaled from Proxima Cen as mentioned before, this does not affect our analysis, as the quiescent UV fluxes are so small compared to the flaring values that uncertainties introduced by using such a scaled spectrum from another M dwarf in the UV range are negligible. The flare peak flux at the effective wavelength of the *Kepler* band can be calculated as

$$F_{\rm Kepler} = \frac{\int F(\lambda) T(\lambda) \lambda \, d\lambda}{\int T(\lambda) \lambda \, d\lambda} \quad (1)$$

where $T(\lambda)$ is the *Kepler* transmission curve taken from the VOSA filter profile service[2] (Rodrigo et al. 2012; Rodrigo & Solano 2020). We want to note that this curve requires to be multiplied by λ in Eq. 1 as it is provided for a photon counter detector. We fix the temperature of the blackbody emission and adjust the relative flare area X until $F_{\rm Kepler}$ matches the observed peak flux. With this solution, we integrated $F(\lambda)$ over the UV ranges of interest to obtain the UV fluxes during the flare peak. Using a relationship between flare peak temperatures and flare energies in the g'-band (Howard et al. 2020),

[2] http://svo2.cab.inta-csic.es/theory/fps/

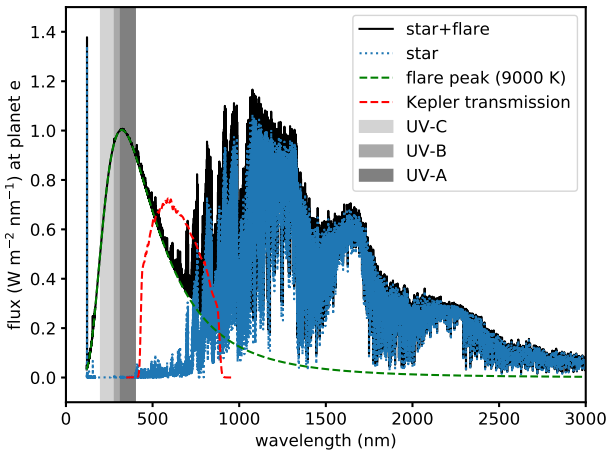

Figure 1. Quiescent stellar spectrum (blue), superflare peak spectrum (green; blackbody with 9000 K), and total spectrum (black) scaled to the orbit of TRAPPIST-1 *e*. The *Kepler* transmission curve is shown in red, and the relevant UV ranges as gray shaded areas.

where we estimate the latter quantity from the integrated white-light energy (Vida et al. 2017) and a scaling factor of 0.19 (Glazier et al. 2020) to convert it to the g'-band, we obtain 8926 K. Therefore, we adopt a value of 9000 K for the superflare peak temperature, which is a typical value for flares on M dwarfs (Hawley & Fisher 1992; Allred et al. 2006; Howard et al. 2018). We note that varying the flare temperature by 10% changes the UV-A, UV-B, and UV-C peak fluxes by about 15, 25, and 40%, respectively.

There are some estimates for flare temperatures of TRAPPIST-1 available, but only for flares with lower energies of $10^{30} - 10^{31}$ erg in the *TESS* band, much lower than the superflare we study here. Howard et al. (2023) estimated the temperatures of four flares on TRAPPIST-1 from near-infrared spectra, ranging between 2900 and 5300 K around the peaks of the flares. On the other hand, the peak temperatures of two flares with similar energies determined with multi-color optical photometry were found to be much higher, about 13620 and 8290 K (Maas et al. 2022). These discrepant results could indicate either a possible large intrinsic spread of flare temperatures for flares of similar energies, consistent with what is seen in the larger sample of flares compiled for different stars by Howard et al. (2020), or that the near-infrared spectra of Howard et al. (2023) only measured a cooler component of the flare emission compared to the optical observations.

As the blackbody emission at typical flare peak temperatures has its emission maximum in the UV, the peak enhancement relative to the quiescent level in this superflare is about a factor of >4000 in the UV-C band, much larger than the factor of five enhancement in the *Kepler* band. The UV-A, UV-B, and UV-C superflare peak fluxes at the respective orbits of the TRAPPIST-1 planets *e*, *f*, and *g* (Gillon et al. 2017) are summarized in Table 1. Figure 1 shows the quiescent stellar spectrum, peak flare spectrum (assumed to be a 9000 K blackbody), and the total (star+flare) spectrum scaled to the orbital distance of planet *e* as an example.

2.2.2 *Flare evolution*

To approximate the UV flux evolution during the superflare, we applied our modeling approach to the total light curve. Because we

Table 1. Quiescent and superflare peak fluxes in the different UV bands for planets e, f, and g for a superflare peak temperature of 9000 K. Orbital distances a of the planets were taken from Gillon et al. (2017). Comparison values for the present Earth are surface fluxes in the case of UV-A and UV-B, for UV-C the flux outside the atmosphere is given because the surface flux is zero (Abrevaya et al. 2020).

planet	a (AU)	activity state	UV-A ($W\,m^{-2}$)	UV-B ($W\,m^{-2}$)	UV-C ($W\,m^{-2}$)
e	0.02817	quiet	0.059	0.0073	0.015
		flare	82.45	34.45	62.04
f	0.0371	quiet	0.034	0.0042	0.0086
		flare	47.54	19.86	35.77
g	0.0451	quiet	0.023	0.0028	0.0058
		flare	32.17	13.44	24.21
Earth	1	quiet	30-50	2	6.27

cannot disentangle the flare's temperature and area with observations in only one photometric band, we fix the temperature at the adopted peak value of 9000 K and fit the corresponding evolution of the flare area along the light curve. Another option would be to fix the flare area and let the temperature vary, but observations show that the temperature typically varies less than the area during a flare (few tens of percent vs. factors of a few; e.g. Hawley et al. 2003), so we choose the first approach. This generally predicts higher flare fluxes than the approach with a fixed area, so we likely obtain an upper limit to the flare emission. In addition, we note that adopting the peak temperature of the flare for the whole evolution overestimates the total UV emission of the flare. Together these two aspects provide a worst-case scenario for the superflare's UV emission.

Similar to the flare peak fitting procedure described in section 2.2.1, we fit every point of the flare light curve with our blackbody model to obtain the evolution of UV emission during the flare. Integrating the resulting time sequence of flare spectra over wavelength and time, we obtained a flare energy from the blackbody emission of 1.4×10^{33} erg. As this radiation component comprises about 60% of the bolometric flare energy (Osten & Wolk 2015), we estimate a total bolometric flare energy of $\sim 2.4 \times 10^{33}$ erg. The resulting UV-A, UV-B, and UV-C light curves obtained by integrating each modeled flare spectrum over the respective bands are shown, in comparison with the optical K2 observation in Fig. 2. The fluxes are shown as scaled to the orbit of planet e; planets f and g receive about 60 and 40%, respectively, of planet e's irradiation (cf. Table 1). The K2 light curve was taken from Vida et al. (2017) and converted from magnitude differences to flux assuming a quiet flux in the *Kepler* band of $0.0217\,W\,m^{-2}$ at a distance of 1 AU, computed using Eq. 1 and the *Kepler* band parameters from the VOSA filter profile service (Rodrigo et al. 2012; Rodrigo & Solano 2020). One can see that the UV fluxes, despite being orders of magnitude lower than the optical during quiescence, are almost comparable during the main phase of the superflare.

2.3 Microorganisms and irradiation conditions

To allow a direct comparison with other studies that intended to determine the biological impact of flares on the surface of TRAPPIST-1 (O'Malley-James & Kaltenegger 2017; Estrela et al. 2020), the model microorganisms that were chosen for our experiments are the same taken as reference in these studies. Those are the bacteria *D. radiodurans* and *E. coli*, regarded as radiotolerant and radiosensitive, respectively. *D. radiodurans* (R1) was cultivated in liquid TGY medium containing (g L^{-1}) tryptone (10); yeast extract (6); glucose (2) (Anderson 1956), with orbital shaking at 200 rpm, at 30°C until the stationary growth phase.

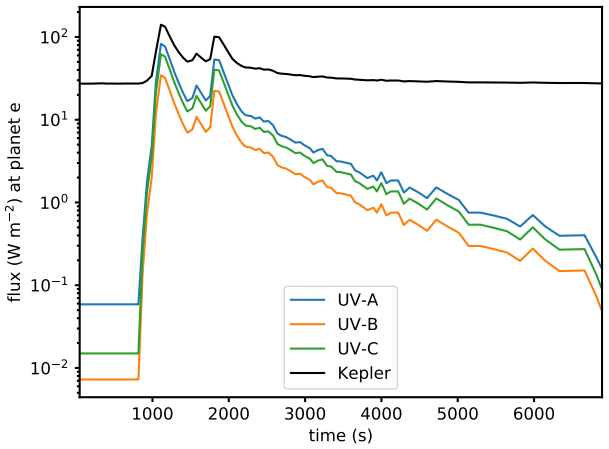

Figure 2. Observed flare light curve in the *Kepler* band (black) in comparison with the modeled UV-A (blue), UV-B (orange), and UV-C (green) curves. The fluxes are scaled to the orbit of planet e, and a flare temperature of 9000 K was assumed.

E. coli K12 MG1655 was cultivated in Luria-Bertani (LB) broth (g L^{-1}) tryptone (10); yeast extract (5); NaCl (5), with orbital shaking at 200 rpm at 37ºC until the stationary growth phase.

The cells were then harvested by centrifugation and the pellets were washed and resuspended with sterile distilled water. The optical density at 650nm (OD) of the bacterial suspensions was adjusted to 0.3 corresponding to a mean concentration of microorganisms of 6.28×10^7 colony-forming units (CFU) per mL for *D. radiodurans* and 6.54×10^8 for *E. coli*.

To study the biological impact of UVR we considered planets e, f, and g of the seven planets of the TRAPPIST-1 system, as they are in the conservative habitable zone. For this study, we focused exclusively on flares given that quiescent UVR fluxes on planets e, f and g are much lower than those at the present Earth. In the case of planet e, the fluxes are 500-800 times lower than the Earth value for UVA, 300 times lower for UVB, and 400 times lower for UVC. These factors are even larger for planets f and g. For UVA and UVB these values would be negligible from the biological point of view as microorganisms on Earth are able to live under much higher fluxes. For UVC these values would be negligible too, however, given that the terrestrial atmosphere blocks this wavelength range, the reference provided by space experiments performed in the low Earth orbit, should be used for comparison. These experiments show that several microorganisms exposed to unattenuated extraterrestrial solar UVR spectrum were able to survive these quiescent fluxes (Cockell et al. 2011; Novikova et al. 2015; Horneck et al. 1994), similar to the case described for Proxima *b* in Abrevaya et al. (2020) (see Table 1).

For our experiments, we focused then on the case of a superflare (see section 2.2), and a fluence rate value of 75 $W\,m^{-2}$ was used for the experiments (see section 2.5 for the calculation of this value). The term "fluence rate" in our study is defined according to Braslavsky (2007) as total radiant power, incident from all directions onto a small sphere divided by the cross-sectional area of

that sphere (SI unit W m^{-2}) From this fluence rate value, different fluences were obtained after irradiating during different time intervals. In this case, the term fluence is defined according to Braslavsky (2007) as the radiant energy, at a given point in space, incident on a small sphere from all directions divided by the cross-sectional area of that sphere (SI unit J m^{-2})

The irradiation source was composed of two low-pressure mercury lamps (Philips TUV15W/G15T8) located 2 cm above the free surface of the bacterial suspensions to reach a fluence rate of 75 W m^{-2}. This value was measured by actinometry using an iodate-iodure solution (Rahn 1997). Aliquots of 10 mL of the bacterial suspensions were placed in Petri dishes (5 cm diameter) and irradiated during different intervals of time under magnetic stirring. In preliminary assays, a slight increase in the temperature of the samples was observed during long irradiations. To avoid this effect the samples were placed on a stainless steel holder cooled by water circulation and maintained at 20ºC during the exposure. The control groups were non-irradiated samples. The irradiation and post-irradiation procedures were performed under sodium light to prevent photoreactivation repair (Phillips SON 70 W E). This condition was selected also as a worst-case scenario where life forms can use only a single repair system (normally microorganisms have a double repair system to remove DNA lesions caused by UVR, with two different mechanisms known as photoreactivation and nucleotide excision repair).

2.4 Counting procedure and data analysis

The counting procedure for *D. radiodurans* has been previously described in Oppezzo et al. (2024). Viable counts for *E. coli* were obtained by applying the same method but using LB plates and incubated for 18 h at 37ºC. A protocol modification was included to increase the limit of detection (LOD) for the highest fluence values, where 8 mL of the irradiated samples were filtered and the filters were transferred to the surface of agar plates and incubated. The survival fraction was then calculated as N/N$_0$, where N is the viable count after an applied fluence H$_0$, and N$_0$ is the viable count of non-irradiated cells. From the calculated values survival curves were obtained by plotting the logarithm of the survival fraction as a function of the applied fluence. A kinetic model was then used to interpret the data in agreement with the one described in Oppezzo et al. (2024). Considering a minimum of 10 CFU per 8 mL of bacterial suspension, the LOD for *D. radiodurans* was estimated in -7.70 and for *E. coli* in -8.47.

2.5 Action spectra of *D. radiodurans* and *E. coli* and equivalent fluences

The action spectra for the microorganisms were obtained using the inactivation rate constants (k_{in}) for different wavelengths in the UVR range. The inactivation rate constants at different wavelengths were reported by Setlow & Boling (1965) for *D. radiodurans*, and by Matsumoto et al. (2022) for *E. coli*. To estimate the values corresponding to the intervals between the wavelengths for which experimental data are available, we considered that the shape of the action spectrum for a given effect depends on the absorption spectra of the chromophores (molecules that absorb light) involved in the occurrence of this effect. Considering this fact, the sum of several partially overlapped absorption bands, with maxima near the wavelengths corresponding to known UV absorption maxima of the nitrogenated bases in the DNA and aromatic amino acids in proteins (i.e. 220, 260, and 280 nm), was used to approximate the action spectrum. The height and width of these bands were adjusted, and some minor bands were added to improve the adjustment of the curve to the experimental data. The resulting action spectra for both microorganisms are shown in Fig. 3.

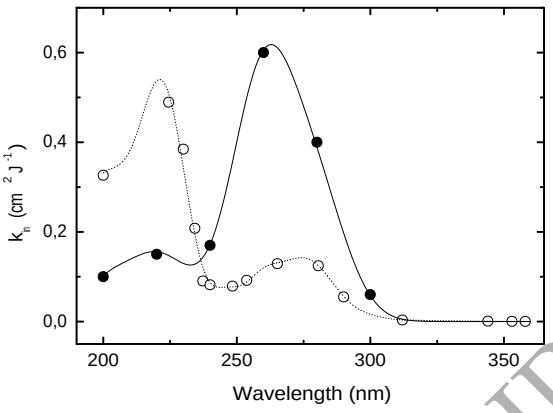

Figure 3. Action spectra obtained in our study. *E. coli* (black circles) and *D. radiodurans* (open circles).

If we consider the lethal action of radiation, a fluence of $1/(k_{in})$ would be required to reduce the population to 1/e (0.37) of its initial value. The relation between the fluence value at a wavelength λ ($H_0(\lambda)$) that produces a given effect and the fluence value at 254 nm ($H_0(254)$) that is expected to make the same effect would be:

$$\frac{H_0(\lambda)}{H_0(254)} = \frac{1/k_{in}(\lambda)}{1/k_{in}(254)} = \frac{k_{in}(254)}{k_{in}(\lambda)} \quad (2)$$

The fluence of radiation at 254 nm equivalent to the one corresponding to the other wavelengths could be calculated as:

$$H_0(254) = \frac{k_{in}(\lambda)}{k_{in}(254)} H_0(\lambda) \quad (3)$$

The ratio between the constants in Equation 3 is called the germicidal factor (GF) (Bolton 2017). By using this equation it was possible to calculate the fluence of germicidal radiation (254 nm) required to produce an effect equivalent to that expected for a fluence of radiation at a different wavelength (in the case of our study UVB and UVC ranges, 200-305 nm, as for 305-400 nm the GF equals zero). Then, each point in time of the reconstructed UV spectrum of TRAPPIST-1 at the orbit of planet e shown in Fig.1 was multiplied by the GF and the results were integrated over the wavelength to estimate the fluence rate at 254 nm that would produce the same lethal effect. As we would have a different GF for each microorganism then the same procedure was applied for *D. radiodurans* and *E. coli* (see Fig. 4). By calculating in this way the equivalence between the fluence imparted in the experiments and the one expected during a flare we are assuming: i) the effect is independent of the fluence rate (the Bunsen-Roscoe reciprocity law is fulfilled, i.e.: the biological effect depends on the total fluence but not on the administration regime (Bunsen R 1855, 1857a,b, 1859); ii) the effects produced by different wavelengths are additive (there are no synergistic or antagonistic actions between them).

The fluence rate value of 75 W m^{-2} used in our experiments was selected after considering the average of the two main flare

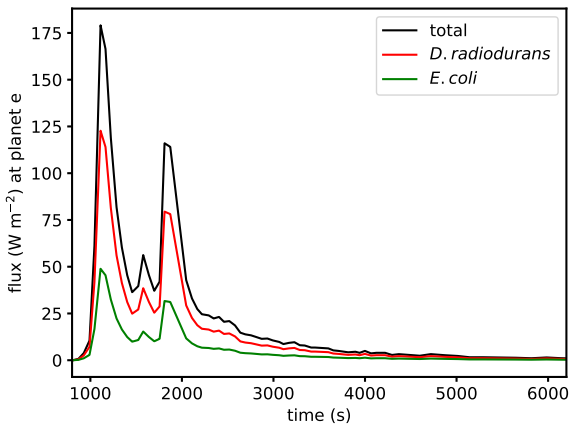

Figure 4. Total UV flux (200-400 nm) for the superflare (black line) at the surface of planet *e*, and equivalent fluxes for germicidal radiation (254 nm) for *E. coli* (green line) and *D. radiodurans* (red line) estimated by using the action spectra of Fig. 3.

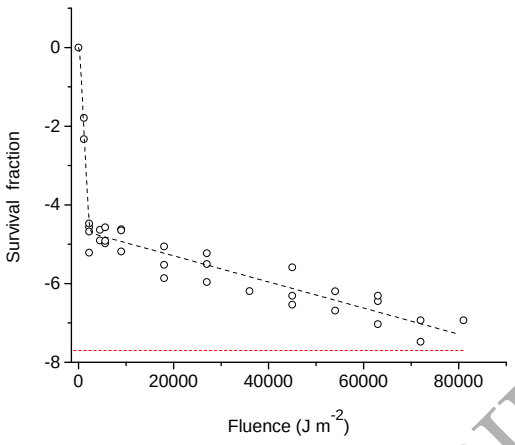

Figure 5. Survival curve obtained for *D. radiodurans* at different fluences of germicidal radiation. The survival fraction is the log (N/N_0). The black line corresponds to a fit obtained with a kinetic model and the red line corresponds to the LOD.

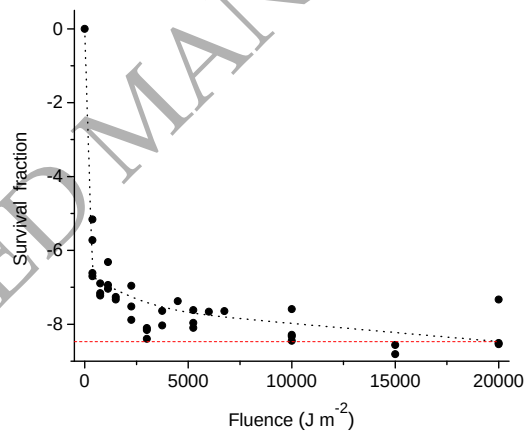

Figure 6. Survival curve obtained for *E. coli* at different fluences of germicidal radiation. The survival fraction is the log (N/N_0). The black line corresponds to a fit obtained with a kinetic model and the red line corresponds to the LOD.

peaks of the equivalent fluxes for both microorganisms (at the surface of planet *e*) in Figure 4. We considered planet e as this would be the one that receives the highest flux of UVR on its surface. As well as, for this estimation we assumed that the microorganisms would also be fully exposed to the UVR flux coming from the superflare without any source of shielding either biological (e.g.: UV shielding provided by clumping, biofilm formation) or environmental (e.g.: UV shielding that could be provided by an atmosphere, or an ocean). This would represent the "worst-case scenario" from the biological point of view. Then, with the information obtained for planet *e*, we estimated the biological impact of UVR on planets *f* and *g*. This is possible because the UVR flux varies proportionally according to the orbital distance (see Table 1). As there is a linear relationship between the flux and the fluence, the UVC fluence estimated for planets *f* and *g* can be estimated from planet *e*.

3 RESULTS

In this study, we evaluated experimentally the biological impact of a superflare on the surface of the TRAPPIST-1 planets *e*, *f*, and *g*, given the superflare case reported by Vida et al. (2017). First, we studied planet *e* because this planet receives the highest UVR flux. As shown in Fig. 4 the flux (fluence rate) of the superflare case under analysis is plotted as a function of the time duration of the event. The integration below the curve of this plot provides an estimation of the fluence that microorganisms would receive on the planet's surface from the superflare, being 113100 J m^{-2} of polychromatic radiation (200 - 400 nm) throughout the entire flare for planet *e*, 65146 J m^{-2} for planet *f*, and 44109 J m^{-2} for planet *g*. By converting this fluence of UV polychromatic radiation produced by the superflare of 113100 J m^{-2}, to the equivalent fluence of germicidal radiation (λ=254nm) that would produce an equivalent biological effect we obtained values of 77330 J m^{-2} for *D. radiodurans* on the surface of planet *e*, 44542 J m^{-2} on the surface of planet *f* and 30159 J m^{-2} for planet *g*. In the case of *E. coli* these values were 30826 J m^{-2} on the surface of planet e, 17756 J m^{-2} on the surface of the planet *f*, and 12022 J m^{-2} on the surface of the planet *g*.

As a result of a series of experiments conducted to test microbial survival after exposure to germicidal radiation up to 81000 J m^{-2}, survival curves were obtained for *D. radiodurans* and *E. coli* shown in Figs. 5 and 6, respectively. The experimental data was fitted with a kinetic model (see Section 2.4).

The survival curve of *D. radiodurans* as depicted in Fig. 5 shows a rapid decay until a fluence of approximately 2000 J m^{-2}, which can be interpreted as the inactivation of cells susceptible to germicidal radiation. At greater fluences, there is a change in the slope that can be interpreted as a subpopulation of cells more tolerant to germicidal radiation. For the fluence values assayed in the experiments (up to 81000 J m $^{-2}$), which exceed the equivalent fluences for the superflare on the surface of planets *e*, *f*, and *g*, calculated in the previous paragraph, the survival fraction remained above the LOD. This means that it would be possible to find sur-

viving cells on the surface of all the planets, representing fractions of the whole population being 6.31×10^{-8} on the surface of planet e, 7.76×10^{-7} on the surface of planet f, and 2.34×10^{-6} on the surface of planet g.

The survival curve of *E. coli* also shows a rapid decay (Fig. 6), in this case for fluences up to approximately 300 J m^{-2}, which as in the previous case is interpreted as the inactivation of cells susceptible to germicidal radiation. Above this fluence value, there is again a change in the slope which may correspond to a subpopulation of cells more tolerant to germicidal radiation. For this microorganism, it was possible to detect survivors up to 20000 J m^{-2}, a value which represents two-thirds of the one estimated for the equivalent fluence for the superflare at the surface of the planet e of 30826 J m^{-2} of germicidal radiation. It is important to note that we were able to count CFU up to 25000 J m^{-2} (between 1 and 2 CFU/mL) in a number much lower than the one imposed by the LOD (see Methods, section 2.4) and therefore they were not considered in the analysis. This example helps to emphasize that the impossibility of observing survivors in the survival curve above a fluence, does not directly imply the lack of surviving cells, but the limit to detect cells based on the technique employed. In any case, the proportion of cells in the subpopulation able to tolerate high fluences of UVR is lower than the one for *D. radiodurans*, which can be expected as *E. coli* is more susceptible to germicidal radiation. For the planets f and g, the equivalent fluence for the superflare at the surface is below the fluence at which the population of *E. coli* was reduced to the limit of detection (20000 J m^{-2}) and therefore is possible to estimate survival fractions for this microorganism which would be of 4.40 x 10^{-9} and 8.5 x 10^{-9}, respectively, being a subpopulation of cells that are more tolerant to germicidal radiation.

4 DISCUSSION

In this study, our conclusions about the tolerance of microorganisms on the surface of planets e, f, and g, on the TRAPPIST-1 system, differ significantly from those obtained by previous authors. For instance, Estrela et al. (2020), based their study on calculations of what they define as the "overall effective UV flux (E_{eff}) that falls in a biological body" which included the action spectra of *D. radiodurans* and *E. coli* and used calculations that employ the F_{10} values taken from literature from experiments done at low fluence rates and fluences. They concluded that for planets with an 'Archaean atmosphere', there would not be survival possible on the surface of the planet e for any of these microorganisms. As was mentioned in the previous paragraphs, our results show that it would be possible to find survivors for both microorganisms, although for *E. coli* the reduction in the population, which is much higher than for *D. radiodurans* does not allow us to estimate which would be the exact fraction, but it is presumed to fall below the value determined for planet f (4.40×10^{-9}), due to planet e being closer to the star. Additionally, they mention that only *D. radiodurans* can tolerate these fluences on the surface of planets f and g, but our results suggest that *E. coli* can tolerate the same fluences, although for this microorganism the survival fraction determined in the experiments is around 2 orders of magnitude below the survival fractions obtained for *D. radiodurans* on the surface of these planets. The fact that *D. radiodurans* have higher survival fractions than *E. coli* at the same fluences, implies that this microorganism would have higher chances of recovering the population to its initial levels.

In the case of oxygenic planets with an ozone layer Estrela et al. (2020) also suggest that *E. coli* could not survive on the surface of planet e, but both bacteria could survive on the surface of planets f and g. This is in coincidence with the argument in the study of O'Malley-James & Kaltenegger (2017) which by using the action spectrum of *D. radiodurans* postulates that for UV-active stars, the lack of a sheltering ozone layer would lead to high UVC levels that would be lethal to most life "as we know it" within minutes to hours of exposure (O'Malley-James & Kaltenegger 2017). However, our results show that the planets do not need to have an ozone layer so that the microorganisms can tolerate these radiation levels on the unshielded planetary surfaces. As we demonstrate in our study, tolerance would be possible for both microorganisms independent of the possibility of having atmospheric shielding as we performed experiments assuming the lack of attenuation (i.e.: fluence values employed in the experiments are those directly emitted by the star reaching the orbit of the respective planets). O'Malley-James & Kaltenegger (2017) also states that the UV surface habitability of planets in the habitable zone of the TRAPPIST-1 system depends critically on the activity of the star and the planet's atmospheric composition, particularly they suggest a dense Earth-like atmosphere with a protective ozone layer for microbial survival. However, our results suggest that microorganisms can tolerate the radiation levels of a superflare without the need for any atmospheric shielding. This would mean that shielding could be beneficial, as it will increase the number of survivors, but is not critical for the survival of the tolerant cells. Additionally, the results of our previous study (Abrevaya et al. 2020) have shown that other atmospheric compositions different than those based in ozone can also provide shielding to the most UV-damaging wavelengths (i.e.: UVC and UVB).

The same applies to the possibility of survival on oceanic planets suggested as hypothetical scenarios by Estrela et al. (2020), because, of course, this also can serve as a shielding for UVR. In this case, they stated that *D. radiodurans* could survive on the surface of the ocean but that *E. coli* could survive only if the microorganisms are protected from UVR 8, 9, and 11 m below the ocean surface in the three planets g, f, and e, respectively. In contrast, our results strongly suggest that a fraction of both microorganisms could withstand the radiation of the superflare even without any shielding, meaning that subpopulations of both *D. radiodurans* and *E. coli* would be able to tolerate the UVR from the superflare. The shielding would only increase the number of survivors as explained in the case of atmospheric shielding.

Based on our laboratory experiments using microorganisms with different tolerance to UV, it is important to note as well that, the particular UV-tolerance features of the microorganisms, meaning tolerant or susceptible to germicidal radiation, do not preclude the possibility of obtaining survival as there are tolerant subpopulations of microorganisms able to withstand high fluences of germicidal radiation in both cases. What will change depending on the nature of susceptibility of the microorganisms is the fraction of the remaining population that can tolerate high fluences. This ultimately can affect the probabilities of either the population's re-growth to the original level or their extinction. The evidence of the survival of the population would be more relevant at planetary scales as it indicates the extinction or survival of the species. The possibility of recovery remains an open issue to be answered in future experiments.

Moreover, the reason for the underestimation of microbial survival obtained in other studies relies upon the kind of approach employed for making the survival calculations. This is based on the E_{eff}, which can only provide information about how effective radiation is in producing a biological effect along different wavelengths but cannot predict survival. Moreover, the E_{eff} is used in combination with values such as the F_{10} provided by experiments

from the literature which were done at much lower fluences than the ones equivalent to a flare or a superflare on the surface of a planet in the TRAPPIST-1 system. This issue is connected with the wrong assumption that the survival curve, and then the microbial survival, would remain invariant along the increase in the fluences, and therefore the F_{10} value as well. However, as we demonstrated in this study, the response (tolerance) of the microorganisms at low fluences does not represent the one of the whole population at much higher fluences, as the initial population is not homogenous from the point of view of the tolerance to UV, and therefore extrapolations of the F_{10} values to estimate the tolerance of microorganisms to fluences outside the experimental range are unreliable.

The existence of subpopulations that are more tolerant to germicidal radiation, which can be seen in the form of 'tails' in the survival curves of microorganisms, has been described in the literature related to the phenomena of microbial persistence or cell clumping (Pennell et al. 2008; Kowalski et al. 2020).

Furthermore, it is important to note that the choice of the wavelength employed for the irradiation should not affect the overall results of our study. If, for example, the use of another wavelength increases the effectiveness of the monochromatic radiation (e.g.:, $k_{in}(\lambda) > k_{in}(254)$), according to Eqs. 2 and 3, the fluence imparted to mimic the lethal effect of polychromatic radiation would be reduced (i.e.: $H_0(\lambda) < H_0(254)$), and the expected effect would be the same. This fact is relevant given that recent studies report a highly effective inactivation of microorganisms in the range of 200 – 235 nm (particularly at 222 nm) in aerosols (e.g. Eadie et al. 2022; Buonanno et al. 2024). Apart from the aforementioned fact, which shows that, in principle, the use of another wavelength would not change the conclusions of our study, irradiation at 222 nm would have a limited impact in the context of our simulated planetary scenario and experimental set-up, as the microorganisms are suspended in an aqueous medium and the radiation of 222 nm is strongly attenuated in this type of media (e.g. Sesti-Costa et al. 2022) (i.e.:in the case of our study UV at 254 nm would be more efficient than at 222 nm). Furthermore, in the emission spectrum of TRAPPIST-1 shown in Fig. 1, the number of photons in the range of 200 – 235 nm is about half that of the one in the range of 235 – 280 nm (2.5×10^{19} photons s^{-1} m^{-2} and 5.1×10^{19} photons $s^{-1}m^{-2}$, respectively). This fact would also limit the contribution of shorter wavelength radiation to the lethal action, even when its effectiveness were higher.

The results from the present study are in agreement with our previous results obtained for Proxima *b* where we demonstrated that microbial tolerance would be possible without any environmental shielding after being exposed to UV fluences equivalent to those they will receive from a flare and a superflare on the surface of the planet (Abrevaya et al. 2020).

5 CONCLUSIONS

Our study provides evidence that approaches used by other authors underestimated the probabilities of survival to UVR of microbial life as we know it in extraterrestrial scenarios, particularly for the case of a superflare on the planets *e*, *f*, and *g* of the TRAPPIST-1 system. Contrary to the conclusions of these previous studies we demonstrated that microbial survival would be possible on these planets without any source of shielding, considering as the only factor the exposure to UV germicidal radiation at fluence values equivalent to those of a superflare case reported in the literature. This applies both for a radiotolerant microorganism as *D. radiodurans* as well as to a susceptible one as *E. coli*, although the fraction of microorganisms surviving this event is several orders of magnitude lower for the latter. This is more critical on the surface of planet *e*, as expected as it will receive the highest UV flux.

The reason for the underestimation of the survival of microorganisms in these previous studies has its origin in the fact of not considering the phenomenon of variability in the tolerance to germicidal radiation inside the same population of microorganisms, observed as a change in the slope of the survival curve at different fluences of germicidal radiation. Therefore, the biological response of the exposure to UVR at high fluences cannot be predicted from values as F_10 obtained at low fluences.

Our results emphasize again the need to perform experiments specially designed to test microbial survival in extraterrestrial conditions such as laboratory simulations dedicated to recreating the specific scenarios under evaluation. Although these experiments also have limitations, they represent a more realistic approximation of the conditions encountered in these distant environments.

Future studies will evaluate the probability of microbial recovery after flares and superflares and therefore if populations of microorganisms would be able to withstand these events allowing the survival of the species, including the effect of repetitive flares.

DATA AVAILABILITY

The data underlying this article will be shared on reasonable request to the corresponding author.

ACKNOWLEDGEMENTS

X.C.A. acknowledges the Austrian Academy of Sciences (ÖAW) for the Joint Excellence in Science & Humanities fellowship grant (2020), and also the Federal Ministry of Education, Science and Research (BMBWF), and the awarding organization OeAD (Austria's Agency for Education and Internationalisation) for the Ernst Mach Follow-up Grant (Ernst Mach Grant, Nachbetreuungsstipendium/EZA, MPC-2023-06322). Partial funding was provided by Proyecto de Unidad Ejecutora IAFE (CONICET) (2016-2021), Argentina. This research was funded in whole, or in part, by the Austrian Science Fund (FWF) [10.55776/P30949, 10.55776/I5711]. For the purpose of open access, the author has applied a CC BY public copyright license to any Author Accepted Manuscript version arising from this submission. This research has made use of the SVO Filter Profile Service "Carlos Rodrigo", funded by MCIN/AEI/10.13039/501100011033/ through grant PID2020-112949GB-I00. G.J.M.L. is a member of the CIC-CONICET (Argentina).

REFERENCES

Abrevaya X. C., Leitzinger M., Nuñez Pölcher P. N., Odert P., Lammer H., Hanslmeier A., 2014, Workshop "Star-Planet Interactions and the Habitable Zone" - CEA - Irfu, France,

Abrevaya X. C., Leitzinger M., Oppezzo O. J., Odert P., Patel M. R., Luna G. J. M., Forte Giacobone A. F., Hanslmeier A., 2020, MNRAS, 494, L69

Agol E., et al., 2021, PSJ, 2, 1

Allred J. C., Hawley S. L., Abbett W. P., Carlsson M., 2006, ApJ, 644, 484

Anderson A., 1956, Food Technol., 10, 575

Becker J., Gallo E., Hodges-Kluck E., Adams F. C., Barnes R., 2020, AJ, 159, 275

Bolton J. R., 2017, IUVA News, 19, 10

Braslavsky S. E., 2007, Pure Appl. Chem., 79, 293
Bunsen R R. H., 1855, Poggendorff´s Annalen, 96, 373
Bunsen R R. H., 1857a, Poggendorff´s Annalen, 100, 43
Bunsen R R. H., 1857b, Poggendorff´s Annalen, 101, 235
Bunsen R R. H., 1859, Poggendorff´s Annalen, 108, 193
Buonanno M., Kleiman N. J., Welch D., Hashmi R., Shuryak I., Brenner D. J., 2024, Scientific Reports, 14, 6722
Burdanov A. Y., et al., 2019, MNRAS, 487, 1634
Burgasser A. J., Mamajek E. E., 2017, ApJ, 845, 110
Castellanos Durán J. S., Kleint L., 2020, ApJ, 904, 96
Cockell C. S., Rettberg P., Rabbow E., Olsson-Francis K., 2011, ISME J., 5, 1671
Cooke G. J., Marsh D. R., Walsh C., Youngblood A., 2023, ApJ, 959, 45
Dobos V., Barr A. C., Kiss L. L., 2019, A&A, 624, A2
Dong C., Jin M., Lingam M., Airapetian V. S., Ma Y., van der Holst B., 2018, Proceedings of the National Academy of Science, 115, 260
Ducrot E., et al., 2018, AJ, 156, 218
Eadie E., et al., 2022, Scientific reports, 12, 4373
Estrela R., Palit S., Valio A., 2020, Astrobiology, 20, 1465
Gaia Collaboration et al., 2018, A&A, 616, A1
Gillon M., 2024, arXiv e-prints, p. arXiv:2401.11815
Gillon M., et al., 2016, Nature, 533, 221
Gillon M., et al., 2017, Nature, 542, 456
Glazier A. L., Howard W. S., Corbett H., Law N. M., Ratzloff J. K., Fors O., del Ser D., 2020, ApJ, 900, 27
Gressier A., Mori M., Changeat Q., Edwards B., Beaulieu J. P., Marcq E., Charnay B., 2022, A&A, 658, A133
Hawley S. L., Fisher G. H., 1992, ApJS, 78, 565
Hawley S. L., et al., 2003, ApJ, 597, 535
Hori Y., Ogihara M., 2020, ApJ, 889, 77
Horneck G., Bucker H., Reitz G., 1994, Adv. Space Res., 14, 41
Howard W. S., et al., 2018, ApJ, 860, L30
Howard W. S., et al., 2020, ApJ, 902, 115
Howard W. S., et al., 2023, ApJ, 959, 64
Ih J., Kempton E. M. R., Whittaker E. A., Lessard M., 2023, ApJ, 952, L4
Kislyakova K. G., et al., 2017, Nature Astronomy, 1, 878
Kowalski W., Bahnfleth W., Raguse M., Moeller R., 2020, J. Appl. Microbiol., 128, 1003
Lim O., et al., 2023, in American Astronomical Society Meeting Abstracts. p. 125.06
Lincowski A. P., Meadows V. S., Crisp D., Robinson T. D., Luger R., Lustig-Yaeger J., Arney G. N., 2018, ApJ, 867, 76
Lincowski A. P., et al., 2023, ApJ, 955, L7
Loyd R. O. P., Shkolnik E. L., Schneider A. C., Richey-Yowell T., Barman T. S., Peacock S., Pagano I., 2020, ApJ, 890, 23
Lustig-Yaeger J., Meadows V. S., Lincowski A. P., 2019, AJ, 158, 27
Maas A. J., et al., 2022, A&A, 668, A111
Matsumoto T., Hoshiai T., Tatsuno I., Hasegawa T., 2022, Water, 14, 1394
Novikova N., Deshevaya E., Levinskikh M., Polikarpov N., Poddubko S., Gusev O., Sychev V., 2015, Int. J. Astrobiol., 14, 137
O'Malley-James J. T., Kaltenegger L., 2017, MNRAS, 469, L26
Oppezzo O. J., Abrevaya X. C., Giacobone A. F., 2024, Photochem. Photobiol., 100, 129
Osten R. A., Wolk S. J., 2015, ApJ, 809, 79
Paudel R. R., Gizis J. E., Mullan D. J., Schmidt S. J., Burgasser A. J., Williams P. K. G., Berger E., 2018, ApJ, 858, 55
Payne R. C., Kaltenegger L., 2024, MNRAS, 530, L13
Peacock S., Barman T., Shkolnik E. L., Hauschildt P. H., Baron E., 2019, ApJ, 871, 235
Pennell K. G., Aronson A. I., Blatchey III E. R., 2008, J App Microbiol, 84, 1084
Pidhorodetska D., Fauchez T. J., Villanueva G. L., Domagal-Goldman S. D., Kopparapu R. K., 2020, ApJ, 898, L33
Rahn R. O., 1997, Photochemistry and photobiology, 66, 450
Rodrigo C., Solano E., 2020, in XIV.0 Scientific Meeting (virtual) of the Spanish Astronomical Society. p. 182
Rodrigo C., Solano E., Bayo A., 2012, SVO Filter Profile Service Version 1.0, IVOA Working Draft 15 October 2012, doi:10.5479/ADS/bib/2012ivoa.rept.1015R
Sesti-Costa R., et al., 2022, Photodiagnosis and Photodynamic Therapy, 39, 103015
Setlow J. K., Boling M., 1965, Biochimica et Biophysica Acta (BBA)-Nucleic Acids and Protein Synthesis, 108, 259
Turbet M., Bolmont E., Bourrier V., Demory B.-O., Leconte J., Owen J., Wolf E. T., 2020, ssr, 216, 100
Van Grootel V., et al., 2018, ApJ, 853, 30
Van Looveren G., Güdel M., Boro Saikia S., Kislyakova K., 2024, A&A, 683, A153
Vida K., Kővári Z., Pál A., Oláh K., Kriskovics L., 2017, ApJ, 841, 124
Wheatley P. J., Louden T., Bourrier V., Ehrenreich D., Gillon M., 2017, MNRAS, 465, L74
Wilson D. J., et al., 2021b, ApJ, 911, 18
Wilson D. J., et al., 2021a, ApJ, 911, 18
Wolf E. T., 2017, ApJL, 839, L1
Zhang Z., Zhou Y., Rackham B. V., Apai D., 2018, AJ, 156, 178
Zieba S., et al., 2023, Nature, 620, 746
de Wit J., et al., 2016, Nature, 537, 69